Three-Coordinate Aluminum Is Not a Prerequisite for Catalytic Activity in the Zirconocene−Alumoxane Polymerization of Ethylene

C. Jeff Harlan,[1a] Simon G. Bott,[1b] and Andrew R. Barron*,[1a]

Contribution from the Departments of Chemistry, Harvard University, Cambridge, Massachusetts 02138, and University of North Texas, Denton, Texas 76203

Received September 30, 1994[⊗]

Abstract: The interaction of $(\eta^5\text{-}C_5H_5)_2ZrX_2$ (X = Me, Cl) with $Al(^tBu)_3$ and alumoxanes $[(^tBu)_2Al\{\mu\text{-}OAl(^tBu)_2\}]_2$ and $[(^tBu)Al(\mu_3\text{-}O)]_n$ (n = 6, 7, 9) has been investigated. The Lewis acid−base complexes $(\eta^5\text{-}C_5H_5)_2Zr(X)(\mu\text{-}X)Al(^tBu)_3$ [X = Me (**1**), Cl (**2**)] have been isolated and characterized by variable temperature NMR spectroscopy. The molecular structure of compound **2** has been obtained by X-ray crystallography, indicating the presence of a $Zr(\mu\text{-}Cl)Al$ moiety. The $Zr(\mu\text{-}Cl)Al$ interaction in compound **2** is compared to the Al−Cl bond in [PPN][$AlCl(^tBu)_3$] (**4**). $[(^tBu)_2Al\{\mu\text{-}OAl(^tBu)_2\}]_2$, which contains two three-coordinate (unsaturated) aluminum centers, shows no reaction with $(\eta^5\text{-}C_5H_5)_2ZrMe_2$ and no catalytic activity toward ethylene polymerization. In contrast, the closed cage compound $[(^tBu)Al(\mu_3\text{-}O)]_6$ reacts reversibly to give the ion pair complex $[(\eta^5\text{-}C_5H_5)_2ZrMe][(^tBu)_6Al_6(O)_6Me]$ (**7**). The temperature dependence of the equilibrium constant K_{eq} has been determined and, hence, the enthalpy and entropy for the formation of complex **7** [$\Delta H = -50(1)$ kJ mol^{-1}, $\Delta S = -156(5)$ J mol^{-1} K^{-1}]. Complex **7** is active as a catalyst for the polymerization of ethylene. Polymerization is also observed for mixtures of $(\eta^5\text{-}C_5H_5)_2ZrMe_2$ with $[(^tBu)Al(\mu_3\text{-}O)]_n$ (n = 7, 9) despite the lack of observable complex formation. A solution structure of **7** is proposed upon the basis of NMR spectroscopy and a comparison with $[(Et_2O)Li]_2[(^tBu)_6Al_6(O)_6Me_2]$ (**8**), formed from the reaction of $[(^tBu)Al(\mu_3\text{-}O)]_6$ with MeLi in Et_2O. Upon the basis of NMR spectroscopy, compound **8** exists as either the *anti* (**8a**) or *syn* (**8b**) isomer as a result of *endo* or *exo* methylation of the aluminum centers. The lithium atoms in compound **8** are formally two-coordinate; however, close *tert*-butyl C−H···Li contacts suggest the presence of agostic stabilization. These results are discussed with respect to the commercial $(\eta^5\text{-}C_5H_5)_2ZrMe_2$−methylalumoxane (MAO) polyolefin catalyst system, and the new concept of "latent Lewis acidity" (Γ_{Al-O}) is proposed to account for the reactivity of the cage hexamer $[(^tBu)Al(\mu_3\text{-}O)]_6$. Crystal data for **2**: orthorhombic, *Pnma*, a = 32.181(9) Å, b = 14.437(4) Å, c = 10.812(3) Å, Z = 4, R = 0.1091, R_w = 0.1165. Crystal data for **4**: monoclinic, $P2_1/n$, a = 15.946(2) Å, b = 18.487(2) Å, c = 16.453(2) Å, β = 110.778(7)°, Z = 4, R = 0.0496, R_w = 0.0512. Crystal data for **8**: orthorhombic, *Pbca*, a = 18.249(8) Å, b = 15.215(6) Å, c = 18.359(9) Å, Z = 4, R = 0.0891, R_w = 0.1190.

Introduction

In spite of the importance of alkylalumoxanes,[2] in particular the methyl derivative (methylalumoxane, MAO), as highly active catalysts and co-catalysts for the polymerization of a wide range of organic monomers,[3,4] their structure and mode of catalytic activity remained ambiguous. The structural picture commonly proposed for alkylalumoxanes, involving Al−O chain and cyclic structures (e.g., **I** and **II**) were inconsistent with the

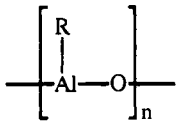

(I)

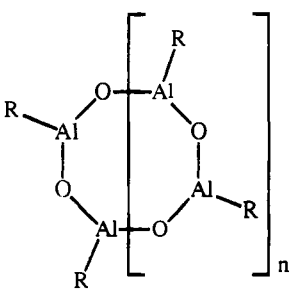

(II)

spectroscopic data available and the known chemistry of aluminum−oxygen compounds.[5] Furthermore, compounds containing three-coordinate aluminum, assumed to be vital for catalytic activity, are rare, only existing in compounds in which oligomerization is sterically hindered by bulky ligands.[6]

The origins of the proposal that alumoxanes must have a structure involving three-coordinate aluminum is best understood by a consideration of the postulated function of methylalumoxane (MAO) in methylzirconocene-catalyzed polymerization of ethylene.[7] Spectroscopic and theoretical data suggest that the role of the Lewis acidic MAO is the abstraction of an alkide, forming a "cation-like" metal center, i.e., eq 1.[8−11] The forma-

* Author to whom all correspondence should be addressed at Department of Chemistry, Rice University, Houston, TX 77251.

⊗ Abstract published in *Advance ACS Abstracts*, May 15, 1995.

(1) (a) Harvard University. (b) University of North Texas.

(2) Alumoxanes are usually defined as species which contain at least one bridging oxo group between two or more aluminum centers. Non-oxo-containing aluminum alkoxides are generally not included in this classification, although alumoxanes may contain a variety of pendant groups attached to aluminum. The term alumoxanes will in the present case, however, denote oligomeric species derived from the hydrolysis of aluminum alkyls, i.e., $[(R_2Al)_2O]_n$ and $(RAlO)_n$.

(3) (a) Vandenberg, E. J. *J. Polym. Sci.* **1960**, *47*, 489. (b) Ishida, S. I. *J. Polym. Sci.* **1962**, *62*, 1. (c) Longiave. C.; Castelli, R. *J. Polym. Sci.* **1963**, *4C*, 387.

(4) See, for example: (a) Sinn, H.; Kaminsky, W.; Vollmer, H. J.; Woldt, R. *Angew. Chem., Int. Ed. Engl.* **1980**, *92*, 390. (b) Sinn, H.; Kaminsky, W. *Adv. Organomet. Chem.* **1980**, *18*, 99.

(5) Pasynkiewicz, S. *Polyhedron* **1990**, *9*, 429.

(6) Healy, M. D.; Barron, A. R. *Angew. Chem., Int. Ed. Engl.* **1992**, *31*, 921 and references therein.

(7) See, for example: Sinn, H.; Kaminsky, W. *Adv. Organomet. Chem.* **1980**, *18*, 99.

0002-7863/95/1517-6465$09.00/0

$$(\eta^5\text{-}C_5H_5)_2Zr(Me)(X) + (MeAlO)_n \rightarrow [(\eta^5\text{-}C_5H_5)_2ZrMe]^+ + [(MeAlO)_n(X)]^- \quad (1)$$

tion of such a cationic zirconium compound has prompted researchers to investigate the activity of other cationic group-4 metal compounds.[12-16] The insistence by many workers that a three-coordinate aluminum center must be present in the catalytically active species developed since compounds with aluminum in a four-coordinate, tetrahedral environment are usually thought not to be Lewis acidic, while compounds with coordinatively unsaturated non-octet three-coordinate aluminum centers are strong Lewis acids.

We have recently reported[17,18] the first conclusive evidence that alkylalumoxanes, prepared by the hydrolysis of AlR_3, have the general formula of $(RAlO)_n$. On the basis of spectroscopic evidence, and confirmed by the X-ray crystallographic structural determinations of $[(^t\text{Bu})Al(\mu_3\text{-}O)]_6$, $[(^t\text{Bu})Al(\mu_3\text{-}O)]_8$ and $[(^t\text{Bu})Al(\mu_3\text{-}O)]_9$, we have shown that these compounds have three-dimensional cage structures, e.g., **III** for $[(^t\text{Bu})Al(\mu_3\text{-}O)]_6$, in which the aluminum centers are four-coordinate and the oxygen coordination environment involves the capping three aluminum atoms. In addition, we have demonstrated that partial hydrolysis of $Al(^t\text{Bu})_3$ allows for the isolation of the tetraalumoxane $[(^t\text{Bu})_2Al\{\mu\text{-}OAl(^t\text{Bu})_2\}]_2$ (**IV**), which is structurally similar to the species that has been proposed to be active in olefin polymerization.[5]

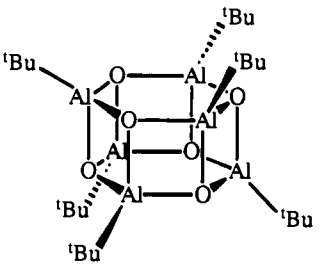

(III)

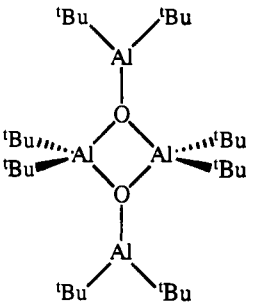

(IV)

Upon the basis of the conventional wisdom, the cage alumoxanes $[(^t\text{Bu})Al(\mu_3\text{-}O)]_n$ should be inactive as co-catalysts with $(\eta^5\text{-}C_5H_5)_2ZrMe_2$, while $[(^t\text{Bu})_2Al\{\mu\text{-}OAl(^t\text{Bu})_2\}]_2$ would be expected to be an active co-catalyst. With the first isolation and structural characterization of alkylalumoxanes, both with and without three-coordinate aluminum centers, we have a unique opportunity to investigate the reactivity of alumoxanes with $(\eta^5\text{-}C_5H_5)_2ZrMe_2$. The results of this study are presented herein.

Results and Discussion

Reaction of $(\eta^5\text{-}C_5H_5)_2ZrMe_2$ with $[(^t\text{Bu})_2Al\{\mu\text{-}OAl(^t\text{Bu})_2\}]_2$. The ^1H NMR spectra of an equimolar mixture of $(\eta^5\text{-}C_5H_5)_2ZrMe_2$ and $[(^t\text{Bu})_2Al\{\mu\text{-}OAl(^t\text{Bu})_2\}]_2$ is of appearance identical to the spectra of the separate compounds and is temperature independent. Addition of excess alumoxane also has no effect on the appearance of the spectra. This result would suggest that the alumoxane, while containing two coordinatively unsaturated three-coordinate aluminum centers, is not sufficiently Lewis acidic to either complex with, or abstract, the methyl group from the zirconium. Because of the *tert*-butyl group substituents on aluminum, it is possible that the steric hindrance at that aluminum precludes methyl abstraction. However, we have previously shown that $[(^t\text{Bu})_2Al\{\mu\text{-}OAl(^t\text{Bu})_2\}]_2$ reacts with pyridine to yield $[(^t\text{Bu})_2Al(py)]_2(\mu\text{-}O)$ (eq 2).[17] Furthermore, this reaction can be followed by ^1H NMR

$$[(^t\text{Bu})_2Al\{\mu\text{-}OAl(^t\text{Bu})_2\}]_2 \xrightarrow{\text{pyridine (xs)}} [(^t\text{Bu})_2Al(py)]_2(\mu\text{-}O) \quad (2)$$

spectroscopy, and the reaction proceeds via initial coordination of pyridine to the three-coordinate aluminum (i.e., $[(^t\text{Bu})_2Al\{\mu\text{-}OAl(^t\text{Bu})_2(py)\}]_2$ in eq 3), subsequent cleavage of the $Al(\mu\text{-}O)_2Al$ unit occurring over a few minutes at room temperature.[19] Given that the cone angle of pyridine complexed to aluminum (*ca.* 85−90°) is comparable to that of a methyl group

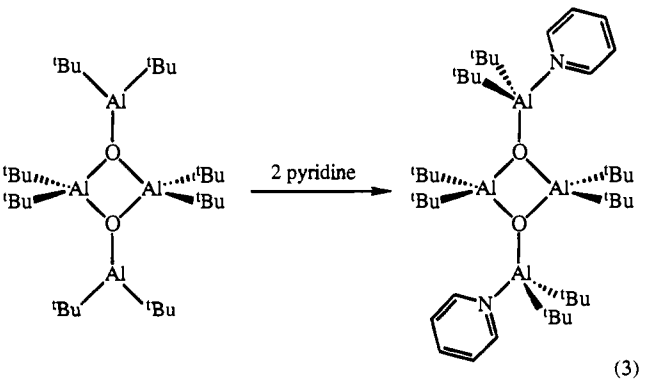

(3)

(8) (a) Sishta, C.; Hathorn, R. M.; Marks, T. J. *J. Am. Chem. Soc.* **1992**, *114*, 1112. (b) Resconi, L.; Bossi, S.; Abis, L. *Macromolecules* **1990**, *23*, 4489.

(9) (a) Jolly, C. A.; Marynick, D. S. *J. Am. Chem. Soc.* **1989**, *111*, 7968. (b) Lauher, J. W.; Hoffmann, R. *J. Am. Chem. Soc.* **1976**, *98*, 1729.

(10) Dahmen, K. H.; Hedden, D.; Burwell, R. L., Jr.; Marks, T. J. *Langmuir* **1988**, *4*, 1212.

(11) Gassman, P. G.; Callstrom, M. R. *J. Am. Chem. Soc.* **1987**, *109*, 7875.

(12) (a) Horton, A. D.; Orpen, A. G. *Organometallics* **1992**, *11*, 8. (b) Horton, A. D.; Orpen, A. G. *Organometallics* **1991**, *10*, 3910. (c) Amorose, D. M.; Lee, R. A.; Petersen, J. L. *Organometallics* **1991**, *10*, 2191. (d) Taube, R.; Krukowka, L. *J. Organomet. Chem.* **1988**, *347*, C9. (e) Eisch, J. J.; Piotrowski, A. M.; Brownstein, S. K.; Gabe, E. J.; Lee, F. L. *J. Am. Chem. Soc.* **1985**, *107*, 7219.

(13) (a) Bochmann, M.; Lancaster, S. J. *J. Organomet. Chem.* **1992**, *434*, C1. (b) Bochmann, M.; Jaggar, A. J. *J. Organomet. Chem.* **1992**, *424*, C5. (c) Bochmann, M.; Karger, G.; Jaggar, A. J. *J. Chem. Soc., Chem. Commun.* **1990**, 1038. (d) Bochmann, M.; Jaggar, A. J.; Nicholls, J. C. *Angew. Chem., Int. Ed. Engl.* **1990**, *29*, 780. (e) Bochmann, M.; Jaggar, A. J.; Hursthouse, M. B.; Mazid, M. *Polyhedron* **1990**, *9*, 2097. (f) Bochmann, M.; Jaggar, A. J.; Hursthouse, M. B.; Motevalli, M. *Polyhedron* **1989**, *8*, 1838. (g) Bochmann, M.; Wilson, L. M.; Hursthouse, M. B.; Motevalli, M. *Organometallics* **1988**, *7*, 1148. (h) Bochmann, M.; Wilson, L. M.; Hursthouse, M. B.; Short, R. L. *Organometallics* **1987**, *6*, 2556. (i) Bochmann, M.; Wilson, L. M. *J. Chem. Soc., Chem. Commun.* **1986**, 1610.

(14) (a) Jordan, R. F. *Adv. Organomet. Chem.* **1991**, *32*, 325. (b) Alelyunas, Y. W.; Jordan, R. F.; Echols, S. F.; Borkowsky, S. L.; Bradley, P. K. *Organometallics* **1991**, *10*, 1406. (c) Jordan, R. F.; Taylor, D. F.; Baenziger, N. C. *Organometallics* **1990**, *9*, 1546. (d) Jordan, R. F.; LaPointe, R. E.; Bradley, P. K.; Baenziger, N. *Organometallics* **1989**, *8*, 2892. (e) Jordan, R. F. *J. Chem. Educ.* **1988**, *65*, 285. (f) Jordan, R. F.; Echols, S. F. *Inorg. Chem.* **1987**, *26*, 383. (g) Jordan, R. F.; LaPointe, R. E.; Bajgur, C. S.; Echols, S. F.; Willett, R. *J. Am. Chem. Soc.* **1987**, *109*, 4111. (h) Jordan, R. F.; Bajgur, C. S.; Dasher, W. E.; Rheingold, A. L. *Organometallics* **1987**, *6*, 1041. (i) Jordan, R. F.; Bajgur, C. S.; Willett, R.; Scott, B. *J. Am. Chem. Soc.* **1986**, *108*, 7410. (j) Jordan, R. F.; Dasher, W. E.; Echols, S. F. *J. Am. Chem. Soc.* **1986**, *108*, 1718.

(15) (a) Yang, X.; Stern, C. L.; Marks, T. J. *J. Am. Chem. Soc.* **1991**, *113*, 3623. (b) Yang, X.; Stern, C. L.; Marks, T. J. *Organometallics* **1991**, *10*, 840.

(16) (a) Hlatky, G. G.; Eckman, R. R.; Turner, H. W. *Organometallics* **1992**, *11*, 1413. (b) Hlatky, G. G.; Turner, H. W.; Eckman, R. R. *J. Am. Chem. Soc.* **1989**, *111*, 2728. (c) Turner, H. W.; Hlatky, G. G. Eur. Pat. Appl. 0 277 004, 1988. (d) Turner, H. W.; Hlatky, G. G. Eur. Pat. Appl. 0 277 003, 1988.

(17) Mason, M. R.; Smith, J. M.; Bott, S. G.; Barron, A. R. *J. Am. Chem. Soc.* **1993**, *115*, 4971.

(18) Harlan, C. J.; Mason, M. R.; Barron, A. R. *Organometallics* **1994**, *13*, 2957.

(19) Mason, M. R.; Barron, A. R. Unpublished data.

(90°),[20] this result would indicate that steric hindrance should not obviate formation of the alumoxane anion. An alternative explanation may be that, if the methyl transfer is a concerted reaction, then the steric hindrance may preclude the close approach of $[(^tBu)_2Al\{\mu\text{-}OAl(^tBu)_2\}]_2$ to $(\eta^5\text{-}C_5H_5)_2ZrMe_2$.

A study of a space filling model based on the literature structures of both reactants[17,21] indicates that formation of a $Zr(\mu\text{-}Me)Al$ unit is not inhibited by the *tert*-butyl groups on $[(^tBu)_2Al\{\mu\text{-}OAl(^tBu)_2\}]_2$. Further evidence is obtained from the isolation of $(\eta^5\text{-}C_5H_5)_2Zr(X)(\mu\text{-}X)Al(^tBu)_3$ (X = Me, Cl).

Reaction of $(\eta^5\text{-}C_5H_5)_2ZrX_2$ (X = Me, Cl) with $Al(^tBu)_3$. The addition of 1 mol equiv of $Al(^tBu)_3$ to $(\eta^5\text{-}C_5H_5)_2ZrX_2$ (X = Me, Cl) yields the air-sensitive Lewis acid–base complex $(\eta^5\text{-}C_5H_5)_2ZrX_2Al(^tBu)_3$ (X = Me (**1**), Cl (**2**)) in near stoichiometric yield. The room temperature ^1H and ^{13}C NMR spectra for compounds **1** and **2** both show a single set of resonances for the cyclopentadienyl and *tert*-butyl ligands. The aluminum *tert*-butyl ^1H NMR resonances [δ 1.22 (**1**), 1.39 (**2**)] are shifted downfield relative to that of uncomplexed $Al(^tBu)_3$ (δ 1.07) but upfield to those of the ionic complexes $[NMe_4][AlCl(^tBu)_3]$ (**3**) (δ = 1.59) and [PPN][$AlCl(^tBu)_3$] [PPN = bis(triphenylphosphine)iminium] (**4**) (δ = 1.50, in C_6D_6). See the Experimental Section for the synthesis of compounds **3** and **4**. We have previously shown[22] that such shifts are consistent with the pyramidalization of the aluminum upon complexation: from trigonal planar in $Al(^tBu)_3$ to pseudotetrahedral in compounds **1** and **2**. In addition, the NMR spectra suggest that distortion from planarity of the aluminum in **2** is greater than in **1**. Given the similarity in steric bulk between $(\eta^5\text{-}C_5H_5)_2ZrMe_2$ versus $(\eta^5\text{-}C_5H_5)_2ZrCl_2$,[23] this change is presumably due to the greater Lewis basicity of the bridging chloride in compound **2**. However, $(\eta^5\text{-}C_5H_5)_2ZrCl_2$ is clearly a worse Lewis base than a chloride ion (see below).

The room temperature ^1H NMR spectrum of $(\eta^5\text{-}C_5H_5)_2ZrMe_2Al(^tBu)_3$ shows a single resonance for the zirconium methyl, δ −0.23. However, upon cooling, this resonance broadens and decoalesces (T_c = 225 K) to give two peaks of equal intensity [δ −0.08 (Zr–Me) and −0.46 (Zr–Me–Al)], consistent with the coordination of the aluminum *via* one of the methyl groups, i.e., $(\eta^5\text{-}C_5H_5)_2Zr(Me)(\mu\text{-}Me)Al(^tBu)_3$. The room temperature spectrum may thus be explained by the presence of the degenerate exchange (eq 4), the activation energy ($\Delta G^{\ddagger}$) of which was calculated to be 41(2) kJ mol^{-1}.

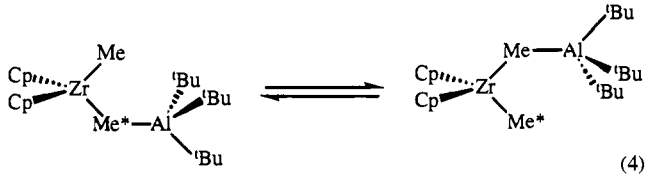

(4)

The fluxionality between the bridging and terminal methyl groups may occur either via dissociation of the $Al(^tBu)_3$ and recoordination or via a concentrated process involving a five-coordinate aluminum transition state. Unfortunately, we are not able to differentiate unambiguously between these two processes since the activation energy for the exchange in eq 4 is only slightly lower than that for the degenerate exchange shown in eq 5 [$\Delta G^{\ddagger}$ = 47(1) kJ mol^{-1}] which must involve dissociation–

$$(\eta^5\text{-}C_5H_5)_2Zr(Me)_2Al(^tBu)_3 + Al^*(^tBu)_3 \rightarrow (\eta^5\text{-}C_5H_5)_2Zr(Me)_2Al^*(^tBu)_3 + Al(^tBu)_3 \quad (5)$$

recoordination of the $Al(^tBu)_3$ moiety.[24] As may be expected this value is significantly smaller than the analogous values determined for complexes with simple Lewis bases, e.g., THF, Et_2O, pyridine, and ketones (56–70 kJ mol^{-1}).[25]

We have no evidence for the formation of an ion pair for either compound **1** or **2**, *c.f.* eq 1. Addition of Lewis bases (THF, MeCN) to compound **1** results in the formation of the new Lewis acid–base complexes $Al(^tBu)_3(L)$ (eq 6), see the Experimental Section.

$$(\eta^5\text{-}C_5H_5)_2Zr(Me)_2Al(^tBu)_3 + L \rightarrow (\eta^5\text{-}C_5H_5)_2Zr(Me)_2 + Al^*(^tBu)_3(L) \quad (6)$$

L = THF (**5**), MeCN (**6**)

The molecular structure of compound **2** has been confirmed by X-ray crystallography, and one of the independent molecules is shown in Figure 1; selected bond lengths and angles are shown in Table 1. The molecular structure of compound **2** consists of a $(\eta^5\text{-}C_5H_5)_2ZrCl_2$ with a $Al(^tBu)_3$ moiety coordinated via a single chloride bridge [Zr–Cl–Al = 151.6(2) and 149.2(3)°]. In both of the crystallographically independent molecules, the

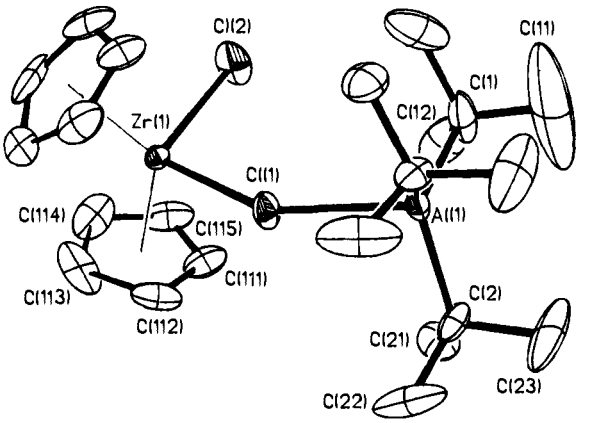

Figure 1. Molecular structure of one of the crystallographic independent molecules of $(\eta^5\text{-}C_5H_5)_2Zr(Cl)(\mu\text{-}Cl)Al(^tBu)_3$ (**2**). Thermal ellipsoids are shown at the 30% probability level, and hydrogen atoms are omitted for clarity.

Table 1. Selected Bond Lengths (Å) and Angles (deg) for $(\eta^5\text{-}C_5H_5)_2Zr(Cl)(\mu\text{-}Cl)Al(^tBu)_3$ (**2**)

Zr(1)–Cl(1)	2.512(5)	Zr(2)–Cl(3)	2.506(5)
Zr(1)–Cl(2)	2.416(7)	Zr(2)–Cl(4)	2.398(6)
Zr(1)–C_{av}	2.47(2)	Zr(2)–C_{av}	2.47(2)
Al(1)–Cl(1)	2.457(7)	Al(2)–Cl(3)	2.475(7)
Al(1)–C(1)	1.99(2)	Al(2)–C(3)	2.07(2)
Al(1)–C(2)	1.98(1)	Al(2)–C(4)	2.06(1)
Cl(1)–Zr(1)–Cl(2)	99.2(2)	Cl(3)–Zr(2)–Cl(4)	98.6(2)
Cl(1)–Zr(1)–Cp	103.9(9)	Cl(3)–Zr(2)–Cp	104.5(9)
Cl(2)–Zr(1)–Cp	104.8(9)	Cl(4)–Zr(2)–Cp	105.6(8)
Cp–Zr(1)–Cp′	115(1)	Cp–Zr(2)–Cp′	114(1)
Cl(1)–Al(1)–C(1)	104.1(8)	Cl(3)–Al(2)–C(3)	101.8(7)
Cl(1)–Al(1)–C(2)	101.4(5)	Cl(3)–Al(1)–C(4)	99.3(5)
C(1)–Al(1)–C(2)	115.4(6)	C(3)–Al(1)–C(4)	116.4(5)
Zr(1)–Cl(1)–Al(1)	149.2(3)	Zr(2)–Cl(3)–Al(2)	151.6(2)

(20) Tolman, C. A. *Chem. Rev.* **1977**, *77*, 313.
(21) Hunter, W. E.; Hrnicir, D. C.; Bynum, R. V.; Penttila, R. A.; Atwood, J. L. *Organometallics* **1983**, *2*, 750.
(22) Barron, A. R. *J. Chem. Soc., Dalton Trans.* **1988**, 3047.
(23) In fact, given the shorter Zr–X and Al–X bond distances in $(\eta^5\text{-}C_5H_5)_2ZrMe_2Al(tBu)_3$ versus $(\eta^5\text{-}C_5H_5)_2ZrCl_2Al(tBu)_3$, greater steric strain would be expected for the methyl compound, **1**.
(24) Shanan-Atidi, H.; Bar-Eli, K. H. *J. Phys. Chem.* **1970**, *74*, 961.
(25) Nash, J. R.; Barron, A. R. National Meeting of the American Chemical Society, Boston, MA, 1990; American Chemical Society: Washington, DC, 1990.

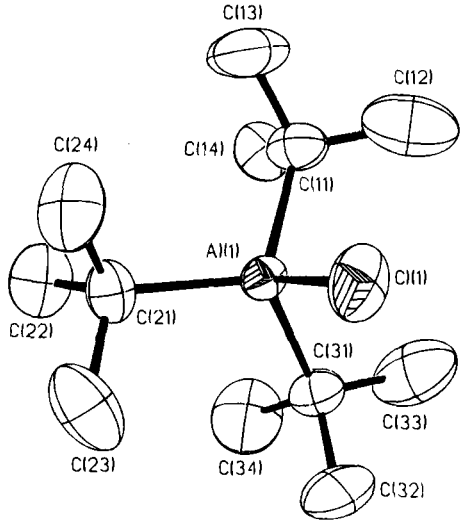

Figure 2. Structure of the aluminum anion in [PPN][AlCl(ᵗBu)₃] (**4**). Thermal ellipsoids are shown at the 30% probability level, and hydrogen atoms are omitted for clarity.

Table 2. Selected Bond Lengths (Å) and Angles (deg) for [PPN][AlCl(ᵗBu)₃] (**4**)

Al(1)−Cl(1)	2.251(3)	Al(1)−C(11)	2.014(7)
Al(1)−Cl(21)	2.003(7)	Al(1)−Cl(31)	2.017(6)
Cl(1)−Al(1)−C(11)	106.5(2)	Cl(1)−Al(1)−C(21)	101.5(2)
Cl(1)−Al(1)−C(31)	106.0(2)	C(11)−Al(1)−C(21)	114.7(3)
C(11)−Al(1)−C(31)	111.2(3)	C(21)−Al(1)−C(31)	115.6(3)

zirconium, chlorides, aluminum, and one of the *tert*-butyl substituents are on a crystallographic mirror plane such that the chlorides exactly bisect the $(\eta^5\text{-}C_5H_5)_2Zr$ wedge. The Zr−Cl distance for the Zr−Cl−Al bridge (av = 2.51 Å) is significantly longer than the terminal Zr−Cl bond (av = 2.41 Å). The latter is close to that observed for $(\eta^5\text{-}C_5H_5)_2ZrCl_2$ (2.43−2.46 Å).[26] The $(\eta^5\text{-}C_5H_5)_2Zr$ unit is opened up *ca.* 14° with respect to uncomplexed $(\eta^5\text{-}C_5H_5)_2ZrCl_2$.

The geometry about aluminum is distorted tetrahedral with the most acute angles being associated with the bridging chloride. The Cl−Al−C angles in the two crystallographic independent molecules of compound **2** [99.3(5)−104.1(8)°] are not significantly smaller than those observed for [PPN][AlCl(ᵗBu)₃] (**4**) [101.5(2)−106.5(2)°], whose structure has also been determined by X-ray crystallography. The structure of the $[AlCl(^tBu)_3]^-$ anion in **4** is shown in Figure 2, and selected structural parameters are given in Table 2. The Al−Cl bond in compound **2** [2.457(7), 2.475(7) Å] is significantly longer than for the chloride salt **4** [2.251(3) Å]. This is consistent with the lower donor ability of the chlorides in $(\eta^5\text{-}C_5H_5)_2ZrCl_2$ compared to a chloride ion. It is also worth noting that the Al−Cl bridge bonds in compound **2** are also longer than previously reported bridging aluminum chlorides (2.20−2.29 Å).[27]

Reaction of $(\eta^5\text{-}C_5H_5)_2ZrMe_2$ with $[(^tBu)Al(\mu_3\text{-}O)]_n$. In contrast to $[(^tBu)_2Al\{\mu\text{-}OAl(^tBu)_2\}]_2$ the coordinatively saturated alumoxane compound $[(^tBu)Al(\mu_3\text{-}O)]_6$ reacts exothermically immediately at room temperature with $(\eta^5\text{-}C_5H_5)_2ZrMe_2$ to yield the methyl transfer product, in equilibrium with $[(^tBu)Al(\mu_3\text{-}O)]_6$ and $(\eta^5\text{-}C_5H_5)_2ZrMe_2$ (eq 7). This equilibrium may be

$$[(^tBu)Al(\mu_3\text{-}O)]_6 + (\eta^5\text{-}C_5H_5)_2ZrMe_2 \rightleftharpoons [(\eta^5\text{-}C_5H_5)_2ZrMe][(^tBu)_6Al_6(O)_6Me] \quad (7)$$
(**7**)

shifted toward the reactants upon cooling. A representative ^1H NMR spectrum of a benzene solution of $[(^tBu)Al(\mu_3\text{-}O)]_6$ and $(\eta^5\text{-}C_5H_5)_2ZrMe_2$ is shown in Figure 3 and clearly shows the presence of two methyl environments ($\delta = 0.71$ and -0.50) in addition to that observed for unreacted $(\eta^5\text{-}C_5H_5)_2ZrMe_2$ ($\delta = -0.13$). Upon the basis of a comparison with other aluminum methyl species including $[(Et_2O)Li]_2[(^tBu)_6Al_6(O)_6Me_2]$ (see below), the peak at −0.50 ppm can be assigned to that of an Al-Me group. The resonance at 0.71 assigned to the zirconium methyl group in **7** is slightly downfield of that observed for the cationic methyl zirconocene compounds, $[(\eta^5\text{-}C_5H_5)_2ZrMe(THF)]^+$ ($\delta = 0.74$). Thus, upon the basis of the NMR spectra (including NOE experiments) and in comparison with $[(Et_2O)Li]_2[(^tBu)_6Al_6(O)_6Me_2]$ (see below), $[(\eta^5\text{-}C_5H_5)_2ZrMe][(^tBu)_6Al_6(O)_6Me]$ (**7**) is proposed to have the structure shown in **V**. The presence of two resonances for the Cp ligands

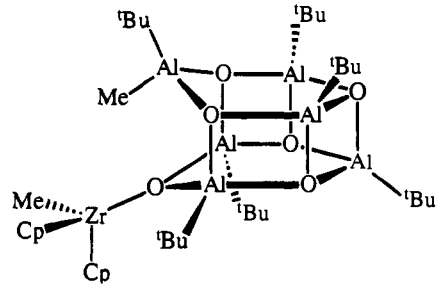

(**V**)

indicates that rotation about the Zr−O bond is slow on the NMR time scale. From a consideration of a model of structure **V**, this is probably due to the steric interactions between the Cp ligands and the *tert*-butyl groups on the alumoxane. Alternatively, the hindered rotation may involve the presence of a Al−Me···Zr interaction. The assignments of the ^1H NMR spectrum is shown in Figure 3.

The formation of a molecular species (or tight ion pair) in benzene and toluene solution is indicated by the concentration dependence of the equilibrium, where higher concentrations promote the formation of $[(\eta^5\text{-}C_5H_5)_2ZrMe][(^tBu)_6Al_6(O)_6Me]$. Furthermore, the equilibrium and formation of $[(\eta^5\text{-}C_5H_5)_2ZrMe][(^tBu)_6Al_6(O)_6Me]$ (**7**) is solvent dependent. While compound **7** is formed in C_6D_6 and C_7D_8, no evidence is observed in CD_2Cl_2, $CDCl_3$, or other polar and/or coordinating solvents that would stabilize ion formation. The close interaction of the zirconium center with the alumoxane cage is further demonstrated by NOE experiments.

The ^1H NMR spectra of toluene-d_8 solutions of $[(^tBu)Al(\mu_3\text{-}O)]_6$ and $(\eta^5\text{-}C_5H_5)_2ZrMe_2$ were obtained at various temperatures (0−35 °C), from which the relative concentrations of $[(^tBu)Al(\mu_3\text{-}O)]_6$, $(\eta^5\text{-}C_5H_5)_2ZrMe_2$, and $[(\eta^5\text{-}C_5H_5)_2ZrMe][(^tBu)_6Al_6(O)_6Me]$ may be calculated and subsequently the equilibrium constants, K_{eq}, determined. From the temperature dependence of the equilibrium constant, ΔH and ΔS were determined, for the formation of $[(\eta^5\text{-}C_5H_5)_2ZrMe][(^tBu)_6Al_6(O)_6Me]$, which were −50(1) kJ mol^{-1} and −156(5) J mol^{-1} K^{-1}, respectively.[28] Addition of $Al(^tBu)_3$ to the equilibrium mixture results in the formation of compound **1** and $[(^tBu)Al(\mu_3\text{-}O)]_6$ exclusively. Thus, $Al(^tBu)_3$ represents a stronger Lewis acid than $[(^tBu)Al(\mu_3\text{-}O)]_6$.

(26) Prout, K.; Cameron, T. S.; Forder, R. A.; Critchley, S. R.; Denton, B.; Rees, G. V. *Acta Crystallogr.* **1974**, *B30*, 2290.

(27) See, for example: (a) Dohmeier, C.; Mattes, R.; Schnökel, H. *J. Chem. Soc., Chem. Commun.* **1990**, 358. Atwood, J. L.; Hrnicir, D. C.; Rogers, R. D. *J. Incl. Phenom.* **1983**, *4*, 199.

(28) Unfortunately re-equilibration of the solution results too rapid to allow the enthalpy ($\Delta H^{\ddagger}$) and entropy ($\Delta S^{\ddagger}$) of activation to be determined from an appropriate Eyring plot.

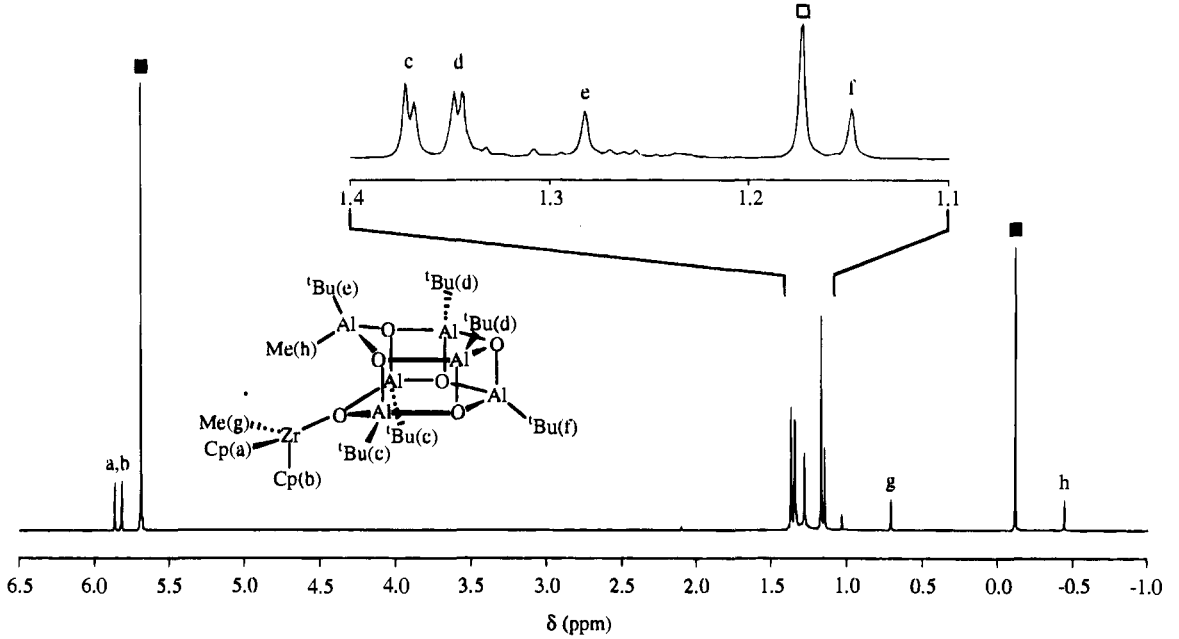

Figure 3. ^{1}H NMR spectrum of $[(^t\text{Bu})_2\text{Al}(\mu_3\text{-O})]_6$ (0.07 mol dm^{-3}) and $(\eta^5\text{-C}_5\text{H}_5)_2\text{ZrMe}_2$ (0.26 mol dm^{-3}) in toluene solution (11 °C). Peaks are assigned and labeled: $[(^t\text{Bu})_2\text{Al}(\mu_3\text{-O})]_6$ (□), $(\eta^5\text{-C}_5\text{H}_5)_2\text{ZrMe}_2$ (■), and $[(\eta^5\text{-C}_5\text{H}_5)_2\text{ZrMe}][(^t\text{Bu})_6\text{Al}_6(\text{O})_6\text{Me}]$ (a–h, see inset).

Table 3. Summary of $(\eta^5\text{-C}_5\text{H}_5)_2\text{ZrMe}_2$–Alumoxane Complex Formation and Co-catalytic Activity for the *tert*-Butylalumoxanes

alumoxane	complex formation[a]	ethylene polymerization[b]
$[(^t\text{Bu})_2\text{Al}\{(\mu\text{-OAl}(^t\text{Bu})_2)\}]_2$	no	no[c]
$[(^t\text{Bu})\text{Al}(\mu_3\text{-O})]_6$	yes	yes
$[(^t\text{Bu})\text{Al}(\mu_3\text{-O})]_7$	no	yes
$[(^t\text{Bu})\text{Al}(\mu_3\text{-O})]_9$	no	yes

[a] From ^{1}H NMR. [b] Alumoxane:$(\eta^5\text{-C}_5\text{H}_5)_2\text{ZrMe}_2$ ratio ≈ 1. [c] No reaction observed for alumoxane:$(\eta^5\text{-C}_5\text{H}_5)_2\text{ZrMe}_2$ ratio ≈ 10.

Unlike $[(^t\text{Bu})_2\text{Al}\{\mu\text{-OAl}(^t\text{Bu})_2\}]_2$, $[(^t\text{Bu})\text{Al}(\mu_3\text{-O})]_7$ (**VI**) and $[(^t\text{Bu})\text{Al}(\mu_3\text{-O})]_9$ (**VII**) are active co-catalysts for the polymerization of ethylene, see Table 3. However, we have been unable to characterize any compounds formed from the interaction with $(\eta^5\text{-C}_5\text{H}_5)_2\text{ZrMe}_2$.

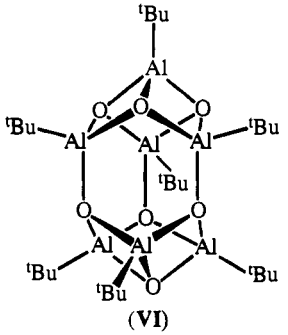

(**VI**)

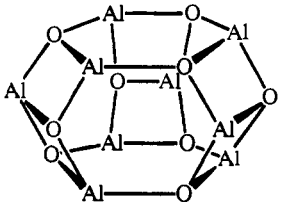

tert-butyl groups omitted for clarity

(**VII**)

Reaction of $[(^t\text{Bu})\text{AlO}]_6$ with MeLi. The reaction of $[(^t\text{Bu})\text{Al}(\mu_3\text{-O})]_6$ with $(\eta^5\text{-C}_5\text{H}_5)_2\text{ZrMe}_2$ may be considered as alkylation of the Al_6O_6 cage. In order to gain further insight into the solution structure of $[(\eta^5\text{-C}_5\text{H}_5)_2\text{ZrMe}][(^t\text{Bu})_6\text{Al}_6(\text{O})_6\text{Me}]$ we have investigated the reaction of $[(^t\text{Bu})\text{Al}(\mu_3\text{-O})]_6$ with MeLi.

Addition of 2 mol equiv of methyllithium in Et_2O/hexane to $[(^t\text{Bu})\text{Al}(\mu_3\text{-O})]_6$ results in the formation of $[(\text{Et}_2\text{O})\text{Li}]_2[(^t\text{Bu})_6\text{Al}_6(\text{O})_6\text{Me}_2]$ (**8**). The ^{1}H NMR of the product mixture from this synthesis shows the presence of two species consistent with the *anti* (**8a**) and *syn* (**8b**) isomers. The former is observed as the major isomer in the solid state, from the X-ray crystallography (see below). While the *syn* isomer is the major species in the mixture, repeated recrystallization favors formation of the *anti* isomer. However, upon standing, a solution enriched in **8a** will re-equilibrate. It is interesting to note that in a mixture of **8a,b** only a single set of resonances is observed in the ^{1}H NMR spectrum for the Et_2O ligands, suggesting that the Et_2O (or possibly the lithium cations) is in rapid exchange.

The molecular structure of compound **8** is shown in Figure 4; selected bond lengths and angles are given in Table 4. Although the ^{1}H NMR of the crystal used for X-ray crystallographic studies shows the presence of both the *anti* (**8a**) and *syn* (**8b**) isomers as major and minor species, respectively, we were unable to refine the structural model as a mixture of isomers (see the Experimental Section). The Al_6O_6 core structure consists of two fused boat conformation Al_3O_3 rings and can be described as being derived from the opening of two opposing edges of a hexagonal prism, see Scheme 1. The

Scheme 1. Structural Relationship between the Al_6O_6 Cages in $[(^t\text{Bu})_2\text{Al}(\mu_3\text{-O})]_6$, $[(\eta^5\text{-C}_5\text{H}_5)_2\text{ZrMe}][(^t\text{Bu})_6\text{Al}_6(\text{O})_6\text{Me}]$ (**7**), and $[(\text{Et}_2\text{O})\text{Li}]_2[(^t\text{Bu})_6\text{Al}_6(\text{O})_6\text{Me}_2]$ (**8**)

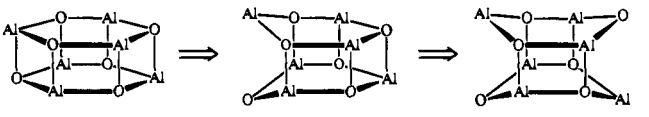

geometries and bond distances around the Al and O atoms are similar to those we have previously reported for other *tert*-butylalumoxane compounds. One unusual feature of the structure, however, is the presence of the linear two-coordinate lithium atoms coordinated to the μ_2-oxides of the Al_6O_6 cage. The Li–O bond distance [1.89(5) Å] is comparable to that observed for Et_2O complexes of three-coordinate lithium [1.910(7) Å].[29] This is a rare example of two-coordinate lithium, previous examples being isolated for dialkyllithium anions, $[\text{LiR}_2]^-$, with sterically hindered alkyl substitutents. The apparent stability of compound **8** may be explained by consideration of the *tert*-butyl methyl···Li distances [2.82–3.05 Å], which are within the range previously observed for agostic

(29) Power, M. B.; Bott, S. G.; Atwood, J. A.; Barron, A. R. *J. Am. Chem. Soc.* **1990**, *112*, 3448.

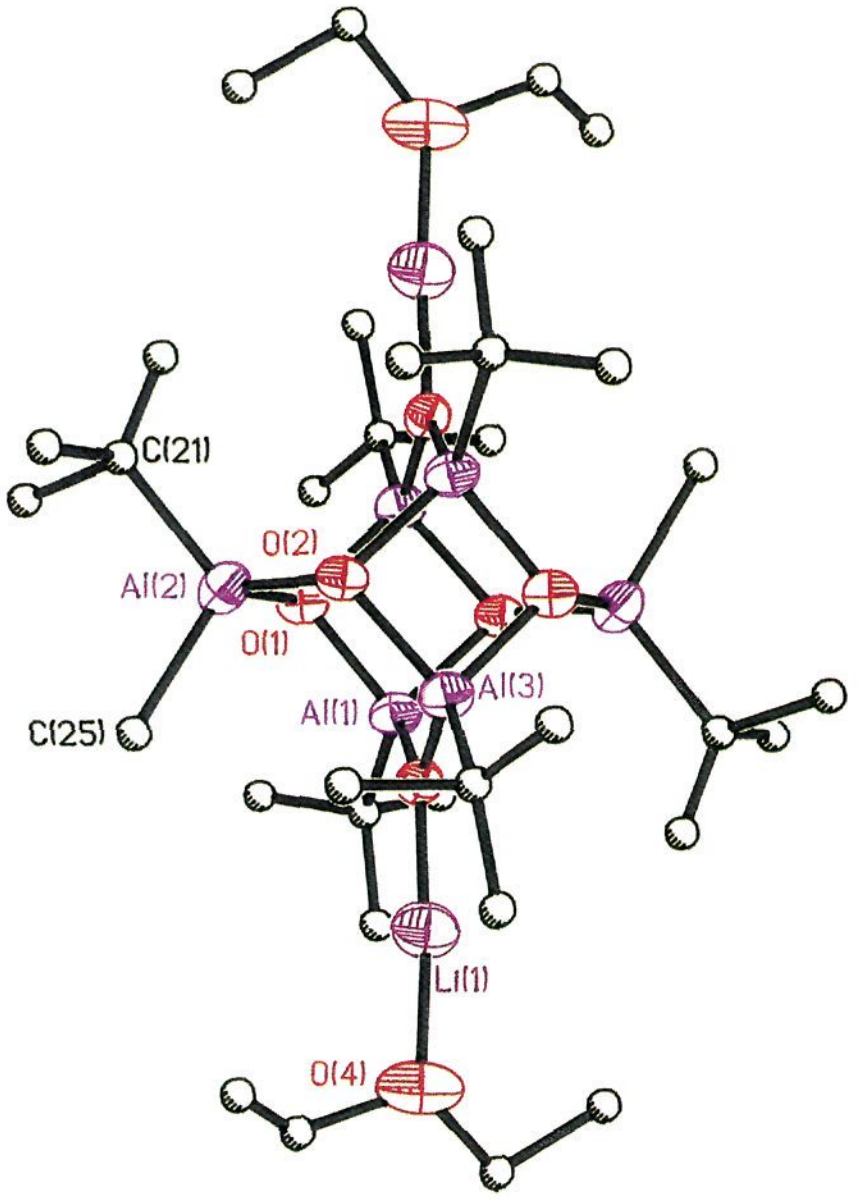

Figure 4. Molecular structure of *anti*-$[(Et_2O)Li]_2[(^tBu)_6Al_6(O)_6Me_2]$ (**8a**). Thermal ellipsoids of carbon atoms are shown at the 30% probability level. Hydrogen atoms are omitted, and carbon atoms are shown as isotropic spheres for clarity.

Table 4. Selected Bond Lengths (Å) and Angles (deg) for $[(Et_2O)Li]_2[(^tBu)_6Al_6(O)_6Me_2]$ (**8a**)

Al(1)−O(1)	1.83(1)	Al(1)−O(2)	1.79(1)
Al(1)−O(3)	1.75(1)	Al(1)−C(11)	2.02(3)
Al(2)−O(1)	1.86(1)	Al(2)−O(2a)	1.81(2)
Al(2)−C(21)	1.95(4)	Al(2)−C(25)	2.07(3)
Al(3)−O(1)	1.78(1)	Al(3)−O(2)	1.82(1)
Al(3)−O(3a)	1.75(1)	Al(3)−C(31)	1.90(3)
Li(1)−O(3)	1.76(5)	Li(1)−O(4)	1.89(5)
O(1)−Al(1)−O(2)	86.8(8)	O(1)−Al(1)−O(3)	109.6(8)
O(1)−Al(1)−C(11)	115(1)	O(2)−Al(1)−O(3)	109.3(8)
O(2)−Al(1)−C(11)	119(1)	O(3)−Al(1)−C(11)	114(1)
O(1)−Al(2)−O(2a)	99.4(8)	O(1)−Al(2)−C(21)	117(1)
O(1)−Al(2)−C(25)	109(1)	O(2a)−Al(2)−C(21)	117(1)
O(2a)−Al(2)−C(25)	109(1)	C(21)−Al(2)−C(25)	103(1)
O(1)−Al(3)−O(2)	87.3(7)	O(1)−Al(3)−O(3a)	109.0(8)
O(1)−Al(3)−C(31)	120(1)	O(2)−Al(3)−O(3a)	108.0(8)
O(2)−Al(3)−C(31)	116(1)	O(3a)−Al(3)−C(31)	112(1)
O(3)−Li(1)−O(4)	172(3)		

interactions (2.69−3.05 Å) but are longer than a Li−C bond (e.g., 2.28 Å in $[LiEt]_4$[30]). The Li···H distances (shortest ≈ 1.9 Å) are shorter than those observed previously (2.1−2.8 Å).[31] The close proximity of the *tert*-butyl methyl groups is clearly seen in the space filling diagram (Figure 5). Thus, we suggest that the lithium atoms are electronically satisfied by two C−H···Li agostic interactions; one from each of two *tert*-butyl groups.[32] The coordination geometry about Li(1) is, therefore,

(30) Dietrich, H. *J. Organomet. Chem.* **1981**, *205*, 291.

(31) (a) Barr, D.; Clegg, W.; Mulvey, R. E.; Smith, R. *J. Chem. Soc., Chem. Commum.* **1984**, 287. (b) Murray, B. D.; Power, P. P. *J. Am. Chem. Soc.* **1984**, *106*, 7011.

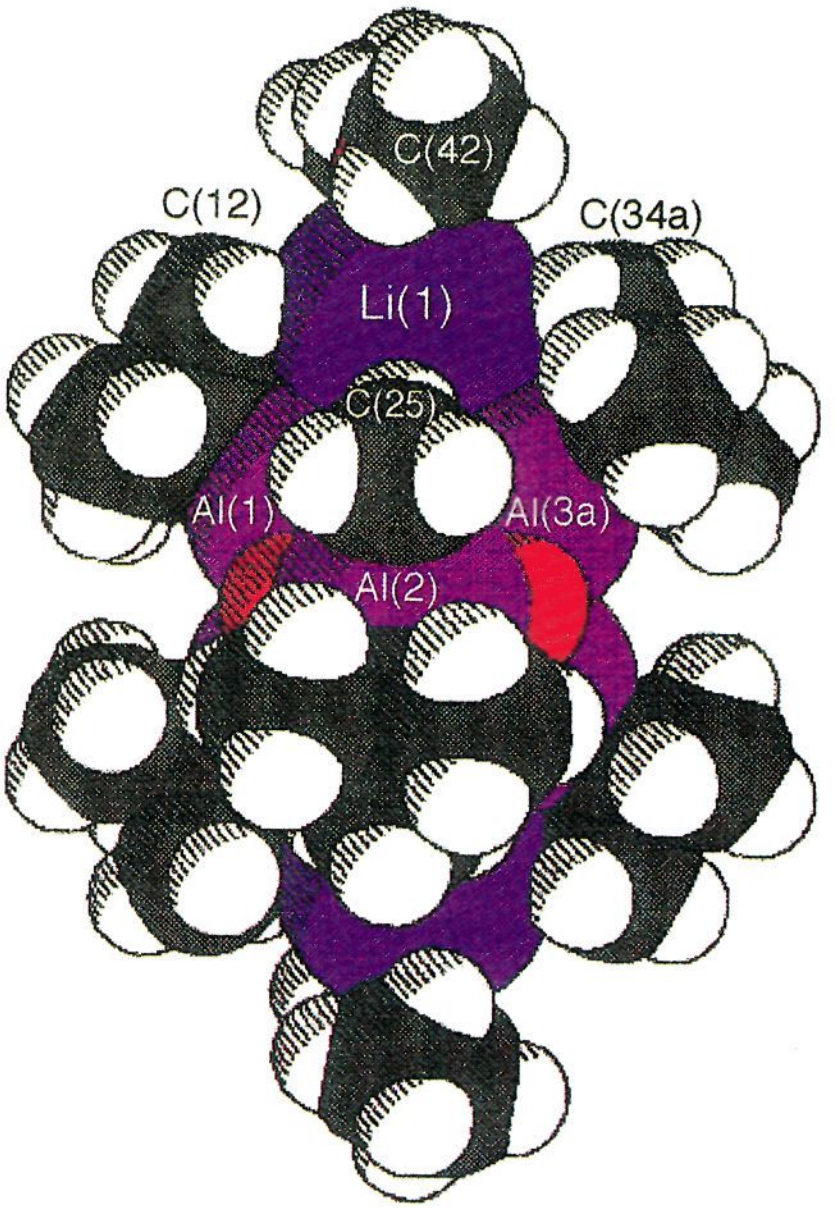

Figure 5. Space filling diagram of *anti*-$[(Et_2O)Li]_2[(^tBu)_6Al_6(O)_6Me_2]$ (**8a**). The close contact of the *tert*-butyl methyl groups, C(12), C(12a), C(34), and C(34a), may clearly be seen.

approximately square planar. It is interesting to note that the O(3)−Li(1)−O(4) angle [172(3)°] is such that the diethyl ether ligand is bent away from the closest *tert*-butyl···Li interaction. Similar distortions have been observed previously for *tert*-butyl···Al interactions.[33]

Ethylene Polymerization. The formation of $[(\eta^5\text{-}C_5H_5)_2\text{-}ZrMe][(^tBu)_6Al_6(O)_6Me]$ from the reaction of $(\eta^5\text{-}C_5H_5)_2ZrMe_2$ with $[(^tBu)Al(\mu_3\text{-}O)]_6$, but no reaction with $[(^tBu)_2Al\{\mu\text{-}OAl(^tBu)_2\}]_2$, may suggest that $[(^tBu)Al(\mu_3\text{-}O)]_6$ should be a co-catalyst for ethylene polymerization. However, it is possible that the "active" cocatalyst is in low (undetectable by ^1H NMR, <1%) quantities or alternatively that the formation of the complex (**7**) is a dead-end route for catalysis. Each of the *tert*-butylalumoxanes, $[(^tBu)Al(\mu_3\text{-}O)]_n$ (n = 6, 7, 9) and $[(^tBu)_2Al\{\mu\text{-}OAl(^tBu)_2\}]_2$, was investigated as co-catalysts for the dimethylzirconocene polymerization of ethylene. It should be noted that all of the alumoxane samples were pure (single species by ^1H NMR), and we have demonstrated that none of the alumoxanes decompose or rearrange in solution even at temperatures higher than those used for catalysis. Thus, we can assume that any variation in catalytic activity is due to the structures of the alumoxanes and not a highly active impurity.

Table 3 summarizes the co-catalytic activity of each of $[(^tBu)Al(\mu_3\text{-}O)]_n$ and $[(^tBu)_2Al\{\mu\text{-}OAl(^tBu)_2\}]_2$ with $(\eta^5\text{-}C_5H_5)_2\text{-}ZrMe_2$. It is interesting to note that $[(^tBu)_2Al\{\mu\text{-}OAl(^tBu)_2\}]_2$ has no catalytic activity, despite having two three coordinate

(32) Agostic interactions have been previously proposed for a number of alkyl lithium compounds. See ref 25.

(33) Healy, M. D.; Power, M. B.; Barron, A. R. *Coord. Chem. Rev.* **1994**, *130*, 63.

Table 5. Summary of Catalysis Data for $[(^t\text{Bu})\text{Al}(\mu_3\text{-O})]_6$ Co-catalyzed Zirconecene Polymerization of Ethene[a]

alumoxane	[amunoxane] (mM)	$[Cp_2ZrMe_2]$ (mM)	Al:Zr ratio	time (min)	yield of polyethylene (g)	relative activity (kg (mol of Zr)$^{-1}$ h^{-1})
$[(^t\text{Bu})\text{Al}(\mu_3\text{-O})]_6$	5.2	5.2	6	60	0.43	4.25
$[(^t\text{Bu})\text{Al}(\mu_3\text{-O})]_6$	30	6.2	24	60	0.24	4.50
MAO[b]	≈32[c]	5.6	≈6	60	*d*	*d*
MAO[b]	≈1250[c]	7.3	≈170	60	3.15	26.8

[a] All polymerization reactions performed at 30 °C, in toluene, at 760 Torr of C_2H_4. [b] Commercial sample (Akzo) *ca.* 9.9 wt % Al in toluene solution. [c] [Al]. [d] None isolated.

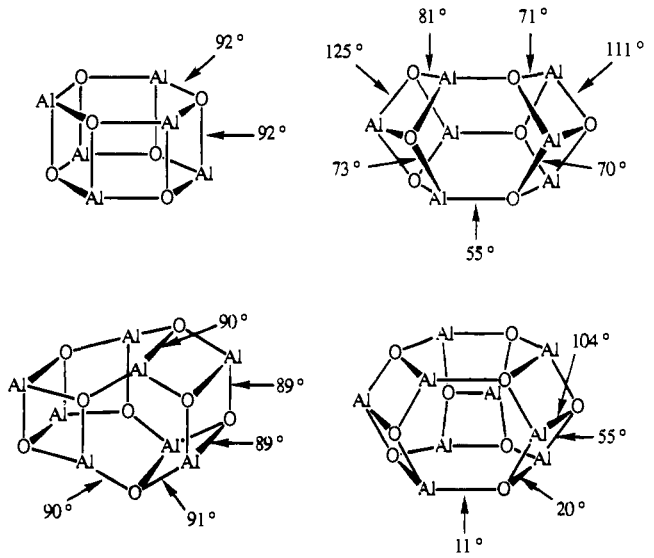

Figure 6. Estimated latent Lewis acidity of individual Al–O bonds in cage alumoxanes, $[(\text{R})\text{Al}(\mu_3\text{-O})]_n$. Alkyl groups have been omitted for clarity.

aluminum centers. On the other hand all the cage compounds are active as polymerization catalysts. In addition, while no complex formation was observed by ^{1}H NMR for either $[(^t\text{Bu})\text{Al}(\mu_3\text{-O})]_7$ or $[(^t\text{Bu})\text{Al}(\mu_3\text{-O})]_9$, they both show catalytic activity.

Addition of a small quantity (*ca.* 2 mol equiv) of ethylene to an equimolar solution of $[(^t\text{Bu})\text{Al}(\mu_3\text{-O})]_6$ and $(\eta^5\text{-}C_5H_5)_2ZrMe_2$ in benzene-d_6 appears not to alter the equilibrium or the speciation; a peak at 5.2 ppm for C_2H_4 is clearly observed. As the solution concentration of ethylene is increased, all of the peaks due to $[(^t\text{Bu})\text{Al}(\mu_3\text{-O})]_6$ and $(\eta^5\text{-}C_5H_5)_2ZrMe_2$ are replaced by peaks due to a mixture of species, similar to those assigned to $[(\eta^5\text{-}C_5H_5)_2ZrMe][(^t\text{Bu})_6Al_6(O)_6Me]$, but all zirconium methyl peaks were absent. In addition, a broad peak consistent with a low molecular weight polyethylene immediately grows in swamping all peaks due to the zirconocene–alumoxane complexes, until polyethylene precipitates from solution.[34] Polyethylene continues to be formed until all the ethylene is consumed. If additional ethylene is added then further polymer is produced.

In Table 5 is a comparison of the relative co-catalytic activity of $[(^t\text{Bu})\text{Al}(\mu_3\text{-O})]_6$ with commercial MAO.[35] The $[(^t\text{Bu})\text{Al}(\mu_3\text{-O})]_6$ is only about one-sixth (16%) as active as commercial MAO under the unoptimized conditions employed.[36] Reasons for the decreased activity of $[(^t\text{Bu})\text{Al}(\mu_3\text{-O})]_6$ compared to MAO are difficult to determine since the exact speciation of MAO is unknown, and they are known to contain significant $AlMe_3$.[37] It is worth noting that, at the lowest Al:Zr ratio (*ca.* 6), $[(^t\text{Bu})\text{Al}(\mu_3\text{-O})]_6$ is active while no polymer could be isolated with MAO as the co-catalyst.[38]

The Latent Lewis Acidity of Alumoxanes. Given the prevalent thinking concerning the activity of alumoxane co-catalysts, the catalytic activity of the cage compounds $[(^t\text{Bu})\text{Al}(\mu_3\text{-O})]_n$ is perhaps surprising. Even more so is the lack of activity for the three-coordinate aluminum compound $[(^t\text{Bu})_2\text{Al}\{\mu\text{-OAl}(^t\text{Bu})_2\}]_2$. This result begs the question: why are the coordinatively saturated cage compounds active catalysts? We propose that while the cage alumoxanes are not themselves Lewis acidic, *per se*, they possess a *"latent Lewis acidity"*, as a consequence of the ring strain present in the cluster.

While as a general concept latent Lewis acidity is useful in explaining the co-catalytic activity of electron-precise cage compounds, it would be desirable to develop a simple model to allow for the prediction of latent Lewis acidity for cage compounds in general and, in particular, for alumoxanes.

If we assume that the latent Lewis acidity of an Al–O bond in a given alumoxane is a function of the ring strain within a cycle, and that four-coordinate aluminum and three-coordinate oxide prefer tetrahedral and trigonal planar geometries, respectively, then we may make a qualitative determination of latent Lewis acidity by calculating the sum of the angular distortions of the cage atoms from this ideal (Γ). Thus, in $[(^t\text{Bu})\text{Al}(\mu_3\text{-O})]_6$, the sum of the intracage angles, $\Sigma(\text{X–E–X})$, for aluminum is 284°, while the ideal value for a tetrahedral geometry is 328.5°; the angular distortion (Γ_{Al}) is therefore ≈ 45°. Similarly, the sum of the intracage angles for oxygen is 312.8° and its Γ_O ≈ 48° (the ideal value being 360°). The strains at aluminum and oxygen are 45° and 48°, respectively, and the total strain (Γ_{Al-O}) is therefore *ca.* 93°. Similar values may be calculated for each of the Al–O bonds in $[(^t\text{Bu})\text{Al}(\mu_3\text{-O})]_n$ (n = 6, 7, 8, 9) (see Figure 6).

Upon the basis of the calculated latent Lewis acidity of the alumoxane cages, the heptamer should be the most reactive of the isolated, *tert*-butyl alumoxanes. However, while catalysis with $(\eta^5\text{-}C_5H_5)_2ZrMe_2$ occurs, no species can be observed by NMR. Why is it therefore that the qualitative measure of latent Lewis acidity does not appear to correlate with the reactivity of $(\eta^5\text{-}C_5H_5)_2ZrMe_2$ with $[(^t\text{Bu})\text{Al}(\mu_3\text{-O})]_n$? Furthermore, the latent Lewis acidity of the hexamer $[(^t\text{Bu})\text{Al}(\mu_3\text{-O})]_6$ and the octamer $[(^t\text{Bu})\text{Al}(\mu_3\text{-O})]_8$ should be essentially identical. While the hexamer readily reacts with $(\eta^5\text{-}C_5H_5)_2ZrMe_2$, the octamer does not appear to do so, although both have co-catalytic activity, why? Of course, there are three possible reasons for these discrepancies in our model for latent Lewis acidity.

First, the latent Lewis acidity does not take the steric hindrance of the Al–O bond into account. As a cage increases in size, the intramolecular distances between the alkyl substitutes generally decreases with a concomitant increase in steric hindrance.[39] However, comparison of the space filling diagrams of $[(^t\text{Bu})\text{Al}(\mu_3\text{-O})]_6$ (Figure 7, top left) and $[(^t\text{Bu})\text{Al}(\mu_3\text{-O})]_8$

(34) No polyethylene is formed for solutions of either $[(^t\text{Bu})\text{Al}(\mu_3\text{-O})]_6$ or $(\eta^5\text{-}C_5H_5)_2ZrMe_2$ independently.

(35) Full details of the *tert*-butylalumoxane-zirconecene-catalyzed polymerization of ethene will be given elsewhere.

(36) It should be noted that no attempt was made to purify the ethene or determine optimum reaction conditions.

(37) We have determined that commercial samples of MAO contain *ca.* 30–40% of "free" $AlMe_3$, see: Barron, A. R. *Organometallics*, in press.

(38) We note that there have been reports for activity in the MAO system using a Zr:Al ratio of 1:12, see: Turner, H. W. US Patent, 4 791 180, 1988 (values in excess of 1:20 are desirable).

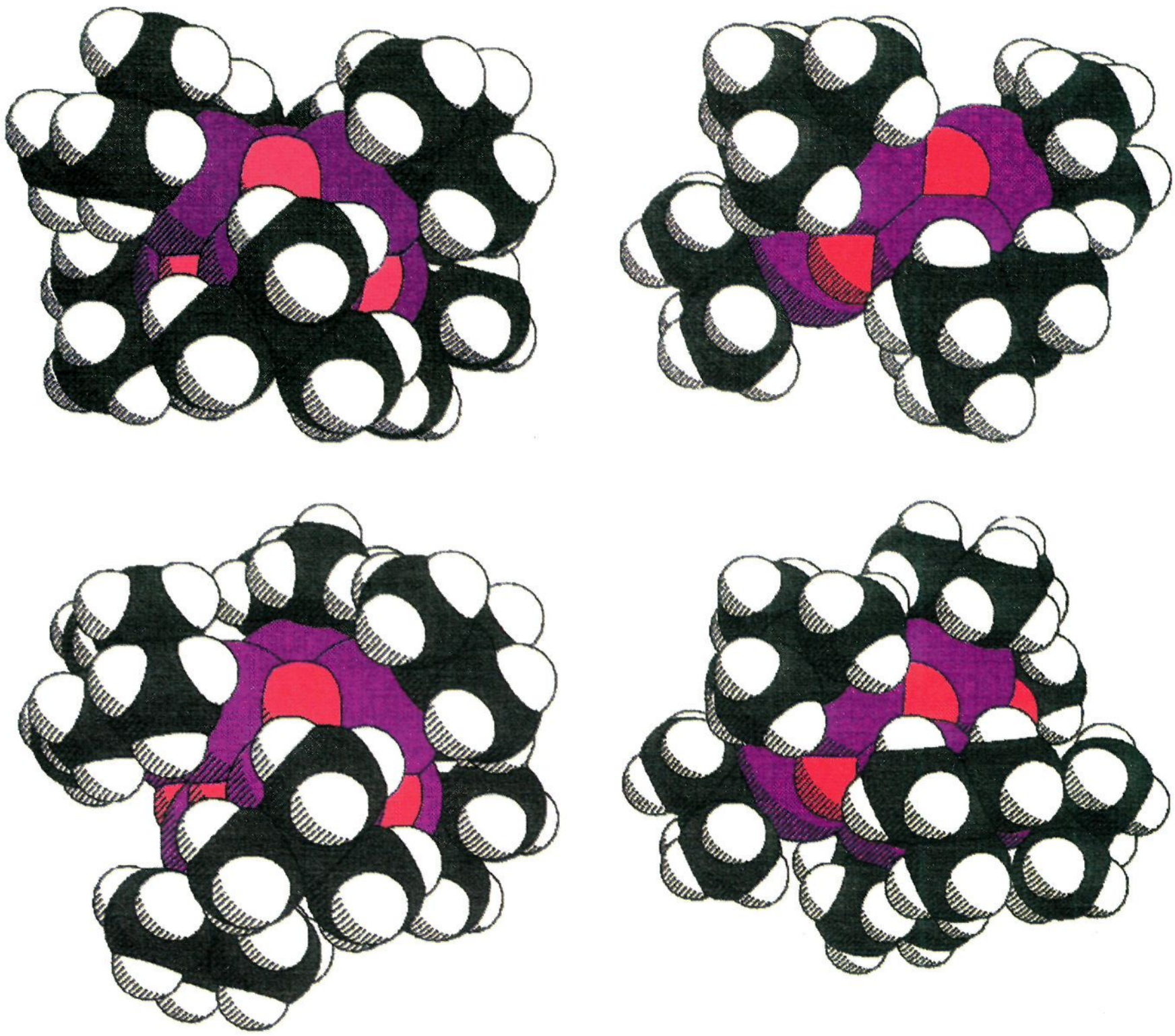

Figure 7. Space filling diagrams of $[(^t\text{Bu})\text{Al}(\mu_3\text{-O})]_6$ (top) and $[(^t\text{Bu})\text{Al}(\mu_3\text{-O})]_8$ (bottom) viewed perpendicular to the Al−O bonds fusing two four-membered rings.

(Figure 7, bottom left) shows that the steric crowding around the Al−O bond is nearly the same, inconsistent with the difference in reactivity. Thus, the steric hindrance of the *tert*-butyl ligand in the cage-opened product must be taken into account. From the alternative space filling diagrams of $[(^t\text{Bu})\text{Al}(\mu_3\text{-O})]_6$ (Figure 7, top right) and $[(^t\text{Bu})\text{Al}(\mu_3\text{-O})]_8$ (Figure 7, bottom right), it can be seen that in $[(^t\text{Bu})\text{Al}(\mu_3\text{-O})]_6$ the *tert*-butyl groups are uncrowded, allowing the cage to open [as is observed for the reaction with $(\eta^5\text{-}C_5H_5)_2ZrMe_2$ and MeLi, above], while in $[(^t\text{Bu})\text{Al}(\mu_3\text{-O})]_8$, the *tert*-butyl groups are sufficiently crowded to hinder cage opening. Thus, in order to predict the reactivity of cages, we must combine the concept of latent Lewis acidity with that of steric hindrance, not only of the alumoxane itself but also of the subsequent cage-opened alumoxane.

Second, using the assumption that latent Lewis acidity is related to the strain in the starting alumoxane does not take into account the possible strain in the ring-opened product. The steric strain in a ring-opened alumoxane may preclude its forming a stable complex. The latter is related to the problem that for certain molecules, e.g., $[(^t\text{Bu})\text{Al}(\mu_3\text{-O})]_6$, the Γ values for the bond fusing two four-membered rings and that fusing one four-membered ring and one six-membered ring are the same (Figure 6). Clearly, experimental data, as shown above, show reactivity at the Al−O bond where the two four-membered rings are fused. This would be predicted on the basis of a consideration of the cage strain in the product. Thus, the reaction observed between $[(^t\text{Bu})\text{Al}(\mu_3\text{-O})]_6$ and both MeLi and $(\eta^5\text{-}C_5H_5)_2ZrMe_2$ forms a new stable six-membered ring, while the alternative reaction, forms a less stable eight-membered Al_4O_4 ring.

Despite these drawbacks, we believe that latent Lewis acidity is a useful concept for explaining the co-catalytic activity of alumoxane cages. We have instigated a detailed physochemical investigation of latent Lewis acidity, and these results will be reported elsewhere.

Conclusions

We have demonstrated that the alumoxanes active as co-catalysts in the zirconocene polymerization of ethylene are three-dimensional cage compounds with four-coordinate alu-

(39) It should be noted that, if as we have shown by multinuclear NMR spectroscopy methylalumoxane (MAO) is a mixture of cage structures, the steric hindrance at any Al−O bond will be less and the reactivity higher. This correlates well with the observed relative reactivity of $[(^t\text{Bu})\text{Al}(\mu_3\text{-O})]_n$ versus MAO, i.e., MAO is approximately 10∼100 times more active than $[(^t\text{Bu})\text{Al}(\mu_3\text{-O})]_n$.

minum centers and not those containing coordinatively unsaturated three-coordinate aluminum centers, as has been traditionally proposed. In order to explain why these electron-precise cage alumoxanes should be active as catalysts, we have developed the concept of latent Lewis acidity, involving the ring strain inherent in small cage compounds. The structure of the product from the reaction of alumoxanes with $(\eta^5\text{-}C_5H_5)_2ZrMe_2$ may be modeled by their reaction with MeLi. The cage-opened compound derived from $[(^t\text{Bu})Al(\mu_3\text{-}O)]_6$, $[(Et_2O)Li]_2[(^t\text{Bu})_6Al_6(O)_6Me_2]$, has been characterized by X-ray crystallography.

Upon the basis of these results, it is clear that we must rethink our view of alumoxanes as co-catalysts. We cannot view their activity as being due to simple Lewis acidity, and the intimate interaction between the alumoxane and the transition metal in an active catalyst suggests that their role may be more than catalysis activation.

Experimental Section

Mass spectra were obtained on a JEOL AX-505 H mass spectrometer operating with an electron beam energy of 70 eV for EI mass spectra. FAB mass spectra were obtained using a JEOL model SX102A mass spectrometer. Spectra were obtained by bombarding the prepared sample with a beam of 6 keV xenon atoms. Infrared spectra (4000–400 cm^{-1}) were obtained using a Nicolet 5ZDX-FTIR spectrometer. IR samples were prepared as mulls on KBr plates. NMR spectra were obtained on Bruker AM-250 and AM-400 (^1H, ^{13}C) spectrometers using (unless otherwise stated) benzene-d_6 solutions. Variable temperature ^1H NMR were obtained on a AM-400 spectrometers. Chemical shifts are reported relative to external TMS (^1H, ^{13}C).

All procedures were performed under purified nitrogen. Solvents were distilled and degassed prior to use. $Al(^t\text{Bu})_3$,[40] $[(^t\text{Bu})Al(\mu_3\text{-}O)]_n$ (n = 6, 7, 9),[17,18] $[(^t\text{Bu})_2Al\{\mu\text{-}OAl(^t\text{Bu})_2\}]_2$,[17] and $(\eta^5\text{-}C_5H_5)_2ZrMe_2$[41] were prepared as previously reported. $(\eta^5\text{-}C_5H_5)_2ZrCl_2$ (Strem Chemicals) was used as received.

$(\eta^5\text{-}C_5H_5)_2Zr(Me)(\mu\text{-}Me)Al(^t\text{Bu})_3$ (1). $Al(^t\text{Bu})_3$ (0.86 g, 4.34 mmol) was added to $(\eta^5\text{-}C_5H_5)_2ZrMe_2$ (1.10 g, 4.38 mmol) in hexane (35 mL) at room temperature, forming a light yellow colored solution from which a yellow precipitate quickly appeared. The reaction mixture was stirred for 3 h and then cooled (0 °C), allowing diamond shaped yellow crystals to form. The crystals were isolated by filtration. Additional product was obtained by concentration and cooling of the supernatant to −24 °C. Yield: 1.6 g, 82%. IR (cm^{-1}): 1261 (w), 1017 (m), 808 (s), 565 (w), 465 (w). ^1H NMR: δ 5.70 (10H, s, C_5H_5), 1.22 [18H, s, $C(CH_3)_3$], −0.23 (6H, s, Zr-CH_3). ^{13}C NMR: δ 111.35 (C_5H_5), 31.97 [$C(CH_3)_3$], 23.52 (Zr-CH_3).

$(\eta^5\text{-}C_5H_5)_2Zr(Cl)(\mu\text{-}Cl)Al(^t\text{Bu})_3$ (2). $Al(^t\text{Bu})_3$ (0.78 g, 3.90 mmol) in toluene (12 mL) was added to a slurry of $(\eta^5\text{-}C_5H_5)_2ZrCl_2$ (1.08 g, 3.9 mmol) in toluene (25 mL) at room temperature. The resultant orange solution was stirred (12 h), and all the volatiles were removed in vacuo. The orange residue was washed with pentane (25 mL), leaving a light yellow solid. The pentane extract was cooled at −24 °C, forming small yellow crystals. The remaining solid was extracted with hexane (70 mL), and the mixture was concentrated and cooled to −24 °C, yielding additional crystalline product. Yield: 0.97g, 54%. IR (cm^{-1}): 1262 (w), 1179 (w), 1017 (s), 934 (m), 816 (s), 729 (m), 575 (s), 415 (s). ^1H NMR: δ 5.82 (10H, s, C_5H_5), 1.39 [18H, s, $C(CH_3)_3$]. ^{13}C NMR: δ 111.35 (C_5H_5), 31.97 [$C(CH_3)_3$].

$[NMe_4][AlCl(^t\text{Bu})_3]$ (3). $[NMe_4]Cl$ (0.54 g, 4.93 mmol) was slurried in toluene (20 mL), and $Al(^t\text{Bu})_3$ (1.24 mL, 4.95 mmol) was added at room temperature. The slurry was stirred overnight. The solvent and volatiles were removed under vacuum, and the residual solid was extracted with toluene (20 mL). The solution was cooled (−24 °C), forming long colorless needles. Yield: 0.53 g, 35 %. MS (negative ion FAB, %): m/z 233 [M^-, 69]. IR (cm^{-1}): 2681 (w), 2677 (w), 1487 (s), 1418 (s), 1174 (w), 1002 (m), 950 (s), 808 (s). ^1H NMR (C_6D_6): δ 1.93 (12H, s, NCH_3), 1.59 [27H, s, $C(CH_3)_3$]. ^{13}C NMR: δ 54.7 (NCH_3), 33.4 [$C(CH_3)_3$], 18.2 [$C(CH_3)_3$].

$[PPN][AlCl(^t\text{Bu})_3]$ (4). [PPN]Cl (2.0 g, 3.48 mmol) was slurried in hexane (70 mL), and $Al(^t\text{Bu})_3$ (0.87 mL, 3.48 mmol) was added at room temperature. The slurry was stirred overnight and the solution filtered. The solid was washed with toluene (30 mL), and volatiles were removed in vacuo. The white solid was extracted with CH_2Cl_2 (25 mL) and filtered off. Pentane (*ca.* 25 mL) was added, forming a two-layer mixture. The mixture was cooled at −24 °C for 2 days, resulting in the formation of large colorless blocks of **6**. Yield: 1.2 g, 45%. MS (negative ion FAB, %): m/z 233 [M^-, 70]. MS (positive ion FAB, %): m/z 538 [M^+, 100]. IR (cm^{-1}): 3057 (w), 2678 (w), 1587 (w), 1483 (m), 1437 (s), 1374 (s), 1324 (br, s), 1274 (s), 1184 (m), 1117 (s), 997 (m), 809 (s), 743 (s), 725 (s), 692 (s), 535 (br, s), 524 (s), 500 (s), 434 (s), 419 (m). ^1H NMR ($CDCl_3$): δ 7.65 (6H, m, *p*-C*H*), 7.44 (24H, m, *o,m*-C*H*), 0.93 [27H, s, $C(CH_3)_3$]. ^{13}C NMR: δ 133.8 (*p*-CH), 132.0 [d, J(P−C) = 7.5 Hz, *m*-CH], 129.5 [d, J(P−C) = 12.5 Hz, *o*-CH], 126.9 [d, J(P−C) = 134 Hz, P−*C*], 32.7 [$C(CH_3)_3$], 17.5 [$C(CH_3)_3$].

$Al(^t\text{Bu})_3(THF)$ (5). THF (1.6 mL, 19.7 mmol) was added to $Al(^t\text{Bu})_3$ (1.26 g, 6.38 mmol) in hexane (20 mL) at room temperature and was stirred for 20 min. The reaction mixture warmed slightly upon addition, and volatiles were removed in vacuo. The white solid was extracted with hexane (20 mL), and the mixture was concentrated and cooled to −24 °C for several hours, forming colorless crystalline needles. Yield: 0.51 g, 30%. MS (EI, %): m/z 198 [M^+ − THF, 45], 141 [$Al(^t\text{Bu})_2$, 100]. IR (cm^{-1}): 423 (s), 568 (s), 808 (s), 854 (s), 928 (m), 1004 (s), 1176 (s), 1357 (m), 1380 (s), 2693 (m). ^1H NMR: δ 3.61 (4H, m, OCH_2), 1.25 [27H, s, $C(CH_3)_3$], 1.00 (4H, m, OCH_2CH_2). ^{13}C NMR: δ 73.5 (OCH_2), 32.9 [$C(CH_3)_3$], 24.7 (OCH_2CH_2), 17.8 [$C(CH_3)_3$].

$Al(^t\text{Bu})_3(MeCN)$ (6). $Al(^t\text{Bu})_3$ (0.79 g, 4.0 mmol) was added to a mixture of MeCN (10 mL) and pentane (70 mL) at 0 °C. The solution was allowed to warm to room temperature and stirred for an additional 1 h. Volatiles were removed in vacuo leaving a fluffy white solid. The solid was dissolved in hexane (30 mL), and the solution was cooled to −24 °C overnight, forming crystalline **4**, which turned to powder on exposure to vacuum. Yield: 0.79 g, 77%. MS (EI, %): m/z 240 [M^+ + H, 5], 198 [$Al(^t\text{Bu})_3$, 70], 141 [$Al(^t\text{Bu})_2$, 100]. IR (cm^{-1}): 2319 (m), 2292 (m), 1262 (w), 1179 (m), 1090 (s), 1003 (s), 938 (3), 810 (s), 571 (s), 420 (s). ^1H NMR: δ 1.31 [27H, s, $C(CH_3)_3$], 0.34 (3H, s, CH_3CN). ^{13}C NMR: δ 119.4 (CH_3CN), 32.2 [$C(CH_3)_3$], 16.5 [$C(CH_3)_3$], 1.06 (CH_3CN).

Reaction of $(\eta^5\text{-}C_5H_5)_2ZrMe_2$ with $[(^t\text{Bu})Al(\mu_3\text{-}O)]_6$. $(\eta^5\text{-}C_5H_5)_2ZrMe_2$ (0.015 g, 59.4 μmol) and $[(^t\text{Bu})Al(\mu_3\text{-}O)]_6$ (0.005 g, 8.3 μmol) were dissolved in toluene-d_8 (0.760 g, 0.806 mL) and transferred to an NMR tube.

$[(\eta^5\text{-}C_5H_5)_2ZrMe][(^t\text{Bu})_6Al_6(O)_6Me]$ (7). ^1H NMR (letter assignments are shown in Figure 3): δ 5.92 (5H, s, C_5H_5, a), 5.87 (5H, s, C_5H_5, b), 1.37 [9H, s, $C(CH_3)_3$, c], 1.36 [9H, s, $C(CH_3)_3$, c], 1.35 [9H, s, $C(CH_3)_3$, d], 1.34 [9H, s, $C(CH_3)_3$, d], 1.28 [9H, s, $C(CH_3)_3$, e], 1.15 [9H, s, $C(CH_3)_3$, f], 0.71 (3H, s, Zr−CH_3, g), −0.50 (3H, s, Al−CH_3, h). ^{13}C NMR: δ 114.41 (C_5H_5, a), 114.06 (C_5H_5, b), 36.3 (Zr−CH_3, g), 33.6, 32.5 [$C(CH_3)_3$, c], 30.7 [$C(CH_3)_3$, e], 30.5, 30.4 [$C(CH_3)_3$, d], 29.4 [$C(CH_3)_3$, f], −9.0 (br, Al−CH_3, h).

$[(Et_2O)Li]_2[(^t\text{Bu})_6Al_6(O)_6Me_2]$ (8). $[(^t\text{Bu})Al(\mu_3\text{-}O)]_6$ (0.56 g, 0.93 mmol) was dissolved in hexane (30 mL), and a MeLi solution (1.33 mL, 1.4 M in Et_2O, 1.86 mmol) was added to the stirring solution, at room temperature. A white microcrystalline precipitate formed immediately. The reaction mixture was stirred for 6 h, whereupon the volatiles were removed in vacuo and the solid was extracted with hexane (60 mL) and filtered. The hexane solution was cooled to −24 °C overnight, and colorless crystals were isolated. Yield: 0.35 g, 48%. Additional product was obtained by extracting the remaining solid with hexane, adding it to the supernatant, concentrating, and cooling. **8a.** ^1H NMR: δ 2.87 [18H, q, J(H−H) = 7.1 Hz, OCH_2], 0.74 [12H, t, J(H−H) = 7.1 Hz, OCH_2CH_3], 1.39 [18H, s, $C(CH_3)_3$], 1.33 [36H, s, $C(CH_3)_3$], −0.45 (6H, s, Al−CH_3). ^{13}C NMR ($CDCl_3$): δ 66.3 (OCH_2), 31.0 [$C(CH_3)_3$], 30.8 [$C(CH_3)_3$], 14.5 (OCH_2CH_3), −8.7 (br, Al-CH_3). **8b.** ^1H NMR: δ 2.87 [18H, q, J(H−H) = 7.1 Hz, OCH_2], 0.74 [12H, t, J(H−H) = 7.1 Hz, OCH_2CH_3], 1.38 [18H, s, $C(CH_3)_3$], 1.35 [18H, s, $C(CH_3)_3$], 1.31 [18H, s, $C(CH_3)_3$], −0.41 (6H, s, Al−CH_3). ^{13}C NMR

(40) (a) Uhl, W., *Z. Anorg. Allg. Chem.* **1989**, *570*, 37. (b) Lehmkuhl, H.; Olbrysch, O.; Nehl, H. *Liebigs Ann. Chem.* **1973**, 708. (c) Lehmkuhl, H.; Olbrysch, O. *Liebigs Ann. Chem.* **1973**, 715.

(41) Samuel, E.; Rausch, M. D. *J. Am. Chem. Soc.* **1973**, *95*, 6263.

Table 6. Summary of X-ray Diffraction Data

compd	$(\eta^5\text{-}C_5H_5)_2Zr(Cl)(\mu\text{-}Cl)Al(^tBu)_3$ (**2**)	[PPN][$AlCl(^tBu)_3$] (**4**)	$[(Et_2O)Li]_2[(^tBu)_6Al_6(O)_6Me_2]$ (**8a**)
empir form	$C_{22}H_{37}AlCl_2Zr$	$C_{48}H_{57}AlClN$	$C_{34}H_{80}Al_6Li_2O_8$
cryst size, mm	0.35 × 0.33 × 0.31	0.42 × 0.57 × 0.58	0.52 × 0.46 × 0.61
cryst syst	orthorhombic	monoclinic	orthorhombic
space group	*Pnma*	$P2_1/n$	*Pbca*
a, Å	32.181(9)	15.946(2)	18.249(8)
b, Å	14.437(4)	18.487(2)	15.215(6)
c, Å	10.812(3)	16.453(2)	18.359(9)
β, deg		110.778(7)	
V, Å^3	5023(3)	4534.8(8)	5098(4)
Z	4	4	4
D(calcd), g/cm^3	1.303	1.131	1.033
μ, mm^{-1}	0.690	0.202	0.163
radiation	Mo Kα (λ = 0.710 73 Å) (graphite monochromator)		
temp, K	298	298	298
2θ range, deg	4.0−45.0	2.0−44.0	4.0−40.0
no. collected	7314	5996	6325
no. ind	3463	5764	3344
no. obsd	3055 ($\|F_o\| > 6.0\sigma\|F_o\|$)	3374 ($\|F_o\| > 6.0\sigma(\|F_o\|$)	949 ($\|F_o\| > 9.0\sigma(\|F_o\|$)
weighting scheme	$\omega^{-1} = \sigma^2(\|F_o\|) + 0.0014(\|F_o\|)^2$	$\omega^{-1} = \sigma^2(\|F_o\|) + 0.04(\|F_o\|)^2$	$\omega^{-1} = \sigma^2(\|F_o\|)$
R	0.1091	0.0496	0.0891
R_w	0.1165	0.0512	0.1190
largest diff peak, e Å^{-3}	1.24	0.23	0.47

($CDCl_3$): δ 66.3 (OCH_2), 31.2 [$C(CH_3)_3$], 30.9 [$C(CH_3)_3$], 30.6 [$C(CH_3)_3$], 14.5 (OCH_2CH_3), −8.9 (br, Al−CH_3).

Polymerization of Ethylene. The polymerization results presented in Table 3 were obtained by bubbling ethylene through a C_6D_6 solution of a weighed quantity of $(\eta^5\text{-}C_5H_5)_2ZrMe_2$ and the appropriate *tert*-butylalumoxane. The reaction was continued until polyethylene precipitated from solution.

The comparative study of MAO and $[(^tBu)_2Al(\mu_3\text{-}O)]_6$ was performed in the following manner: A weighed quantity of $(\eta^5\text{-}C_5H_5)_2ZrMe_2$ (see Table 5) was dissolved in toluene, and the appropriate alumoxane (see Table 5) was added as a toluene solution. Ethylene was bubbled through the solution at 25 °C (760 Torr). After 60 min, the reaction was quenched using methanol and the white polymer was collected and dried.

Crystallographic Studies. Crystals of compounds **2** and **8** were mounted in glass capillaries attached to the goniometer head of the Harvard University Department of Chemistry's Nicolet R3m/V four-circle diffractometer. Data collection using the Nicolet P3 program unit cell and space group determination was all carried out in a manner previously described in detail.[42] A semiempirical absorption correction and Lorentz and polarization corrections were applied to all data. The structures were solved using the direct methods program XS,[43] which readily revealed the positions of the Zr, Al, O, Cl (**2**), Li (**8**), and the majority of the C atoms. Subsequent difference Fourier maps eventually revealed the positions of all of the non-hydrogen atoms for all structures. After all of the non-hydrogen atoms were located and refined anisotropically, the difference map revealed some but not all of the hydrogen atom positions. Organic hydrogen atoms were placed in calculated positions {$U_{iso}(H) = 1.2[U_{iso}(C)]$; $d(C-H) = 0.96$ Å} for refinement. All hydrogen atoms were fixed in the final refinement. Neutral-atom scattering factors were taken from the usual source.[44] Refinement of positional and anisotropic thermal parameters led to convergence (see Table 6). In the case of compound **8**, the *anti* isomer could readily be discerned from the difference map; however, the ^1H NMR spectrum of the crystal indicated that the *syn* isomer should also be present. While several peaks close to the aluminum methyl group, C(25), are present in the difference map, no chemically reasonable solution could be obtained. It is a result of the possible disorder between the two isomers that the resulting *R* and R_w were high and the methyl carbon thermal ellipsoids large. Furthermore, the anisotropic refinement of non-hydrogen atoms resulted in large thermal parameters for the diethyl ether and *tert*-butyl groups. Attempts to refine disorder in a manner similar to that previously described[45,46] did not lead to chemically reasonable solutions.

A crystal of compound **4** was sealed in a glass capillary under argon and mounted on the goniometer of the University of North Texas Department of Chemistry's Enraf-Nonius CAD-4 automated diffractometer. Data collection and cell determinations were performed in a manner previously described.[17] The locations of the majority of non-hydrogen atoms were obtained by using Multan,[47] while the remaining atomic coordinates were determined through the generation of difference Fourier maps using SHELX-76.[48] Hydrogen atoms were included with fixed thermal parameters and constrained to "ride" upon the appropriate atoms [$d(C-H) = 0.95$ Å]. A summary of cell parameters, data collection, and structure solution is given in Table 6. Scattering factors were taken from ref 44.

Acknowledgment. This work was carried out under the auspices of a grant from the Office of Naval Research (Chemistry). Additional financial support was provided by Akzo (Dobbs Ferry, NY) and the Aluminum Research Board.

Supplementary Material Available: Full listings of bond length and angles, atomic coordinates, positional parameters, isotropic and anisotropic thermal parameters, and hydrogen atom parameters (38 pages); tables of calculated and observed structure factors (88 pages). This material is contained in many libraries on microfiche, immediately follows this article in the microfilm version of the journal, can be ordered from the ACS, and can be downloaded from the Internet; see any current masthead page for ordering information and Internet access instructions.

JA9432123

(42) Healy, M. D.; Wierda, D. A.; Barron, A. R. *Organometallics* **1988**, *7*, 2543.

(43) Nicolet Instruments Corp., Madison, WI, 1988.

(44) *International Tables for X-Ray Crystallography*; Kynoch Press: Birmingham, U.K., 1974; Vol. 4.

(45) For refinement of disordered *tert*-butyl groups, see: Power, M. B.; Barron, A. R. *J. Chem. Soc., Chem. Commun.* **1991**, 1315.

(46) For refinement of disordered diethyl ether groups, see: Apblett, A. W.; Barron, A. R. *J. Crystallogr. Spectrosc. Res.* **1993**, *23*, 529.

(47) Main, P.; Fiske, S. J.; Hull, S. E.; Lessinger, L.; Germain, G.; Declerq, J. P.; Woolfson, M. N. Multan 80. A system of computer programs for the authentic solution of crystal structures from X-ray diffraction data. University of York, England, 1980.

(48) Sheldrick, G. M. SHELX. A System of Computer Programs for X-Ray Structural Determination, Cambridge University, 1976.